FINAL TRANSPORT AND FOCUSING FOR THE H I B A L L HEAVY ION FUSION CONCEPTUAL REACTOR STUDY*

I. Hofmann and I. Bozsik

IPP 0/47 July 1981

MAX-PLANCK-INSTITUT FÜR PLASMAPHYSIK

8046 GARCHING BEI MÜNCHEN

MAX-PLANCK-INSTITUT FÜR PLASMAPHYSIK

GARCHING BEI MÜNCHEN

FINAL TRANSPORT AND FOCUSING FOR THE H I B A L L HEAVY ION FUSION CONCEPTUAL REACTOR STUDY*

I. Hofmann and I. Bozsik

IPP 0/47 July 1981

*Diese Arbeit wurde durch das Bundesministerium für Forschung und Technologie gefördert.

IPP 0/47

I. Hofmann

I. Bozsik

Final Transport and Focusing for the HIBALL Heavy Ion Fusion Conceptual Reactor Study

July 1981

A final transport scenario is presented which transports beams of heavy ions from the accelerator to the target within the framework of the HIBALL * (Heavy Ion Beams and Lithium Lead) ICF reactor study. The study considers a total energy of 4.8 MJ to be delivered on a 3 mm radius target within 20 nsec using 20 beams of Bi^{+2} at 10 GeV kinetic energy. The physics of imploding bunches in long periodic transport lines (~ 600 m) is discussed and an appropriate lattice capable of transporting a maximum particle current of 1200 A is defined. A final focusing system with superconducting quadrupoles is suggested, which performs focusing over 8.5 m standoff distance. The influence of chromatic and geometric aberrations on the spot size is discussed. Within the target chamber a vacuum propagation mode is adopted and it is shown that stripping losses are below 5% for the background Pb pressure consistent with HIBALL (~ 10^{-5} Torr at time of beam injection).

*HIBALL is a joint study between the German Heavy Ion Fusion Research Program and the University of Wisconsin.

Contents:

Overview

Transport of beams from the accelerator to the target chamber and focusing on a small target are key issues in heavy ion fusion. Their solution determines to a great deal parameters of the accelerator scenario. The option of transporting beams ballistically in nearly vacuum - without neutralization - has been recognized as a major advantage of using heavy ions and will be considered here. The alternative use of a plasma channel for final transport of heavy ions - similar to light ion fusion schemes - requires considerable additional theoretical and also experimental work before it can be assessed in a reactor design.

One of the main goals of HIBALL is to demonstrate the compatibility of nearly vacuum propagation with the cavity design. In HIBALL wall protection is achieved by a wetted wall scheme, called INPORT concept (Inhibited Flow-Porous Tube Concept). The basis of this new design idea is to use tubes of woven SiC to contain the flow of liquid Lithium-lead alloy ($Li_{17}Pb_{83}$, which yields a tritium breeding ratio of 1.25 for this design). At the outside of the porous tubes the alloy forms a film roughly 1 mm thick, which is sufficient to absorb the energy from X-rays and target debris; several banks of tubes form the 2 m thick blanket, which moderates considerably the neutron flux and reduces the total damage and damage rate in the first solid wall.

After each pellet ignition and vaporization of 13 kg of Lithium-lead due to X-rays, it takes 200 msec to bring the cavity pressure from 10^{2} Torr down to 10^{-5} Torr by condensation and pumping of noncondensable gases. This final pressure is almost the equilibrium pressure above the coolant at the outlet temperature of 500^{o} C. Under these circumstances it is found that beam loss by stripping of Bi^{+2} on Pb gas can be kept below 5%; neutralization by stripping of the background gas is negligible.

Details of the HIBALL design will be presented in the main HIBALL report (University of Wisconsin Report UWFDM-450 and Kernforschungszentrum Karlsruhe Report No.3202). HIBALL parameters relevant to the final transport scenario are summarized as follows:

Ion type	Bi^{+2}
Ion energy	10 GeV
Beam energy on target	4.8 MJ
Maximum power	240 TW
Pulse length	20 nsec
Number of beams	20
Emittance p.beam	120 mm-mrad (vertical)
	30 mm-mrad (horizontal)
Maximum particle current p.beam	1.2 kA
Focused spot diamter	6 mm
Distance final focusing magnet - target	8.5 m

A crucial cavity design parameter that determines final transport is the stand-off distance of final focusing magnets from the target (8.5 m). Because of limited space the number of beam lines (included shielding) is confined to approximately ten on a circumference, hence the use of two rows of beam ports demands for a particle current per beam line of the order of 1 kA. It was also felt that elliptic entry ports (with noticeably vertical elongation) rather than circular entry ports of the same area could be advantageous to the design of coolant tubes and possible be helpful for correcting geometric aberrations of the final magnets; hence a ratio of 4:1 was chosen for vertical and horizontal emittances.

The task of the accelerator to produce high beam intensity within a six-dimensional phase space volume small enough to be focused on a 3 mm radius target at reactor stand-off distance (8.5 m) with a pulse duration of 20 nsec has been addressed in the following scenario:

- A RF linear accelerator to achieve the final energy of 10 GeV for Bi^{+2} at a current level of 150 mA; this choice benefits from the high level of confidence in design reliability and cost estimates for RF accelerator technology.
- A large radius transfer ring and several more compact condenser and storage rings to raise the current by almost three orders of magnitude by a sequence of stacking and bunching procedures.
- Induction linear accelerators in the final beam lines supplying a ramped voltage of several hundred MeV to achieve a final ten-fold compression on their long path (2/3 of a kilometer) to the target chamber; this raises the particle current per beamlet from 120 A to 1200 A, hence 20 beamlets per cavity will produce a power of 240 Terawatt on target.

In section 1 the general theory is outlined, whereas section 2 - 3 are dedicated to the specific transport design for HIBALL.

1. General Theory

1.1 Introduction

In addition to cavity related constraints there are beam dynamics limitations which have to be incorporated into the final transport design. Space charge plays an important role here and is a novel feature compared with designs of existing high energy beam lines that usually have negligible space charge effects. The current transport limit in the long periodic beam line connecting with the accelerator is not serious as long as low charge states are chosen (q = 1, 2). In fact, recent computer simulations have shown (see 1.2 and Ref.3) that under certain conditions there is no limit to the transportable current from the physics point of view. Electrostatic repulsion in the final drift can be controlled by increasing the beam divergence, hence the entry port radius. The lens aperture is limited, however, by spherical aberrations and it was felt that a 10 - 20% increase of divergence over the emittance controlled divergence would be reasonable. From the standpoint of aberrations the emittance and momentum spread should be as small as possible. For constant target requirements this is possible only on the expense of the accelerator size. A reasonable compromise has been found somewhere around 60 π mm-rad average horizontal-vertical emittance and 1/2 - 1% momentum spread.

As to the level of confidence one may have into transverse transport considerations we note that computer simulation studies performed at the Naval Research Laboratory and at the Max-Planck-Institut für Plasmaphysik with different codes have led to excellent agreement and also confirm predictions from analytic theory. The situation is different with regard to longitudinal dynamics and longitudinal-transverse coupling under strong space charge conditions during longitudinal compression, which require future work. For the present study a first-order approach has been made by using the longitudinal envelope equation.

1.2 Transverse Stability of Periodic Transport

Beam transfer from the storage rings to the target chamber requires a length of the order of a kilometer to perform longitudinal bunch implosion. It is necessary to ensure transport over a large number of periods of a quadrupole alternating gradient focusing lattice without emittance dilution.

For zero intensity the requirement for stable trajectories is $\sigma_o < 180^o$, with σ_o the phase advance per focusing period, to avoid a half-integer resonance with the focusing period. For finite intensity the defocusing space charge force depresses the tune to a value $0 < \sigma < \sigma_o$ and as a new phenomena collective modes of oscillation can be in resonance with the focusing period, which may lead to emittance growth unless σ_o and σ are constrained to stable bands.

Analytic theory [1] and computer simulation [2)3)] have suggested that instability of the envelope mode is suppressed if $\sigma_o \leqq 90^o$, and instability of the "third order" mode if $\sigma_o \leqq 60^o$. This "third order" mode is evolving with three arms in $x\text{-}p_x$ or $y\text{-}p_y$ phase space and is quite insensitive to the type of distribution function (Fig. 1-1.)

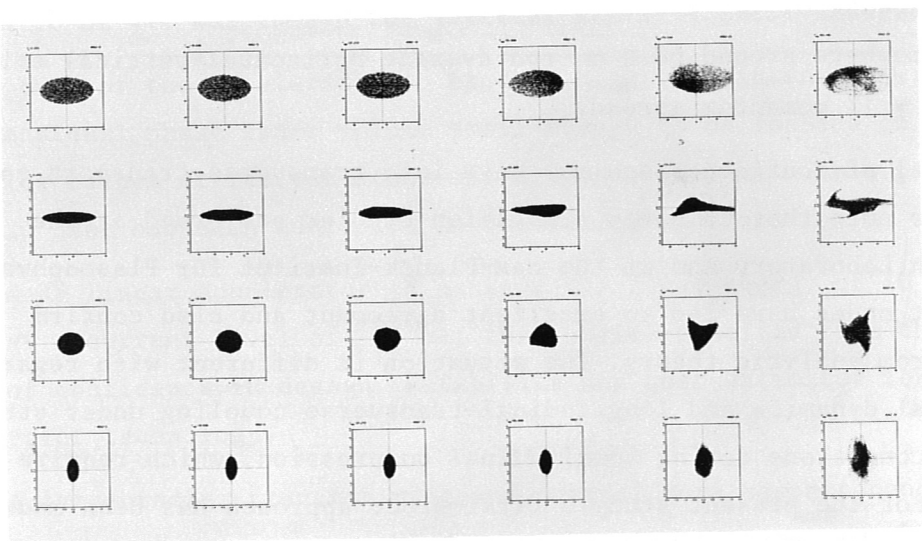

Fig. 1-1. Evolution of initial K-V distribution in periodic FODO focusing with $\sigma_o = 90^o$ and $\sigma = 45^o$ transported over 25 cells ("third order" instability). Shown are projections into $x\text{-}y$, $x\text{-}v_x$, $y\text{-}v_y$ and $v_x\text{-}v_y$ phase planes (from above).

The remaining higher order mode instabilities do not spoil the r.m.s. emittance if σ is depressed to small values [3].

Different emittances in the horizontal and vertical planes may give rise to emittance transfer. The underlying mechanism is a space charge induced coupling instability and requires considerable energy anisotropy and strong tune depression [3]. In most cases the onset of instability is suppressed if strong tune depression is avoided, for instance $\sigma/\sigma_o \gtrsim 0.3$ in both planes for $\varepsilon_x/\varepsilon_y = 4$ (see fig. 1-2. with linear current ramp to simulate bunch implosion). This limits the current performance compared with equal or almost equal emittances, where no limit has been found so far.

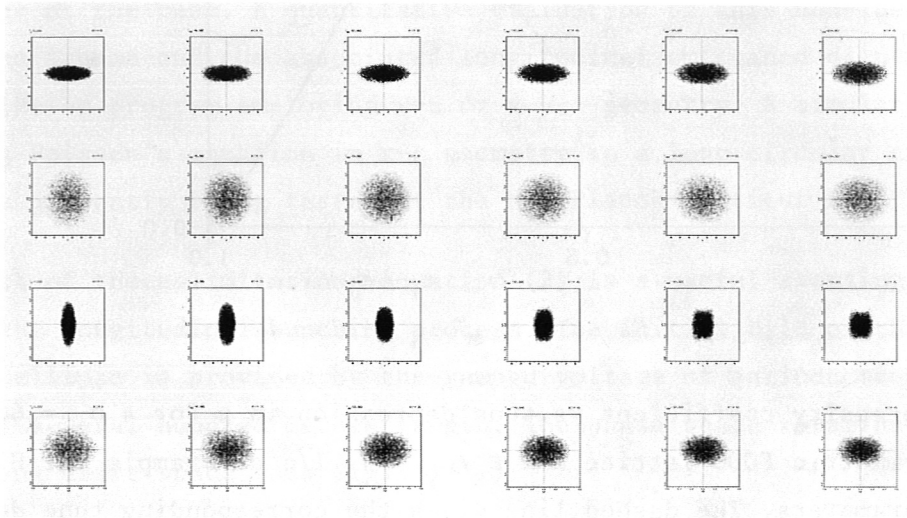

Fig. 1-2. Evolution of initial waterbag distribution in FODO with $\sigma_o = 60^o$ and current ramp depressing tunes from 55^o to 36^o in x and 50^o to 18^o in y over 80 cells. Nearly adiabatic behaviour.

It is convenient to express the current in the channel in terms of the scaled space charge parameter Q' and maximum amplitude u_m (see Ref.4)

$$(1)\quad I/q = 3.66 \cdot 10^6 \, A^{1/3}/q^{4/3} B_Q^{2/3} \, (\beta\gamma)^{7/3} \, \varepsilon^{2/3} \, Q'/u_m^{2/3} \quad [A]$$

where $Q'/u_m^{2/3}$ (Laslett's "figure of merit") is a function of the tune depression σ/σ_o (see Fig. 1-3.) and the remaining quantities are

A	atomic weight
q	charge state
B_Q	pole tip field (Tesla)
β	v/c
ε	unnormalized emittance [m-rad] (for unequal emittances the larger one)

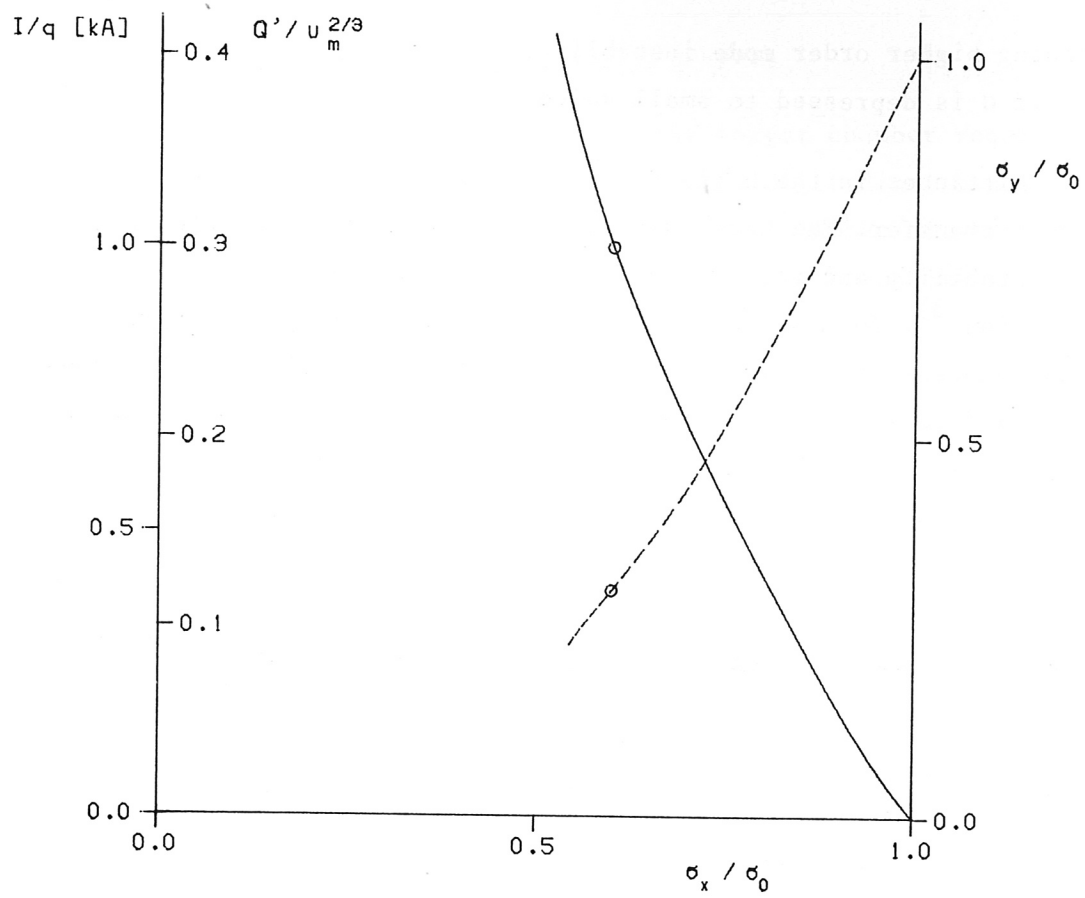

Fig. 1-3. Intensity coefficient vs.tune depression in x for a $\sigma_o = 60^o$ symmetric FODO lattice and $\varepsilon_x/\varepsilon_y = 4$. I/q as example for HIBALL parameters. The dashed line gives the corresponding tune depression in y and the circles indicate stability limits beyond which emittance transfer is possible.

1.3 Longitudinal Bunch Compression

Longitudinal drift bunching is described by an envelope equation [4]

$$(2) \quad z_m'' = \frac{\varepsilon^2}{\gamma^4 z_m^3} + \frac{3}{2}\frac{q^2}{A}\frac{g}{\beta^2\gamma^5}\frac{Nr_p}{z_m^2}$$

with

z_m envelope in z

ε $\frac{1}{\pi}$ × emittance in $(z, \frac{\Delta p}{p})$

N total number of ions

r_p classical proton radius (= $1.52\ 10^{-18}$ m)

Equation (2) assumes a linear space charge force, i.e. parabolic line charge density. This assumption is consistent with a particular distribution function (see Ref.5), whereas in practice deviations from the linear force compression must be expected due to the presumably Gaussian shaped distribution function. In addition, the geometry factor g depends on the transverse position. For a uniform density beam of radius a in a pipe with radius b

$$(3) \quad g = 1 + 2\,\ell n\,(b/a) - (r/a)^2$$

hence it varies between $1 + 2\,\ell n\,(b/a)$ and $2\,\ell n\,(b/a)$ from the center to the edge of the beam. A quantitative evaluation of this non-ideal compression scheme and the associated longitudinal emittancd dilution requires a simulation program employing r-z or x-y-z geometry. A simulation code solving Poisson's equation in r-z geometry in a long circular cross section pipe is presently being tested at the Max-Planck-Institut für Plasmaphysik.

In spite of these limitations equation (2) is a useful starting point to describe the longitudinal bunching process. The initial tilt of the phase space ellipse is provided by the ramped voltage of an induction linac section of several hundred meters length. The phase space rotation is completed in a long drift space (see Fig. 1-4.).

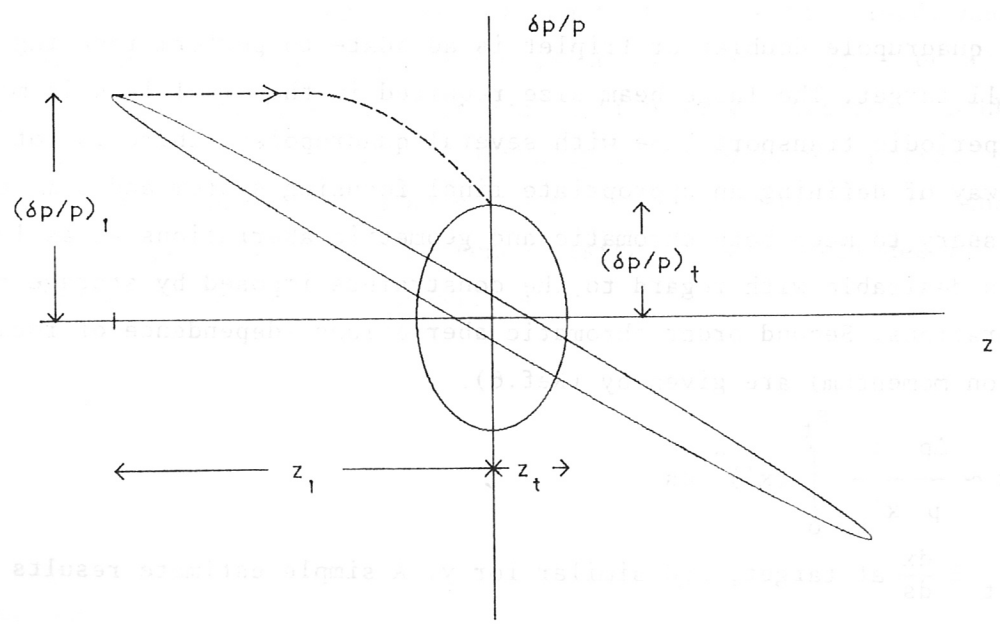

Fig. 1-4. Ellipse rotation in longitudinal phase space for longitudinal bunch implosion under space charge conditions

Assuming constant longitudinal emittance during bunching the coherent initial momentum spread $(\Delta p/p)_i$ necessary to achieve the desired final pulse length can be easily derived from equation (2) by carrying out an integration (see Ref.4). For large compression ratio we have

$$(4)\quad (\Delta p/p)_i^2 = (\Delta p/p)_t^2 + 3\,\frac{q^2}{A}\,\frac{g}{\beta^2\gamma}\,\frac{Nr_p}{z_t}$$

Note that the incoherent momentum spread at target $(\Delta p/p)_t$ is reduced below $(\Delta p/p)_i$ because of space charge repulsion which becomes effective close to the end of the bunching process, when the line charge density has almost come to its final high value.

The necessary drift length is approximately given by

$$L \sim \gamma^2 z_i/(\Delta p/p)_i$$

$(\Delta p/p)_t$ is limited by chromatic aberrations of the final focusing system. The final momentum transmission of a long beam line with bending sections will set a limit to $(\Delta p/p)_i$, but it is assumed here that the final focusing constraint on $\Delta p/p$ is more stringent and thus determines the momentum width in the storage rings.

1.4. Final Focusing Constraints

A final quadrupole doublet or triplet is adequate to perform focusing onto the small target. The large beam size required in the final lens is matched to the periodic transport line with several quadrupoles. There is not a unique way of defining an appropriate final focusing system and some thought is necessary to keep both chromatic and geometric aberrations at as low a level as desirable with regard to the constraints imposed by storage ring considerations. Second order chromatic aberrations (dependence of focal length on momentum) are given by (Ref.6).

$$(5)\quad \Delta x \sim \frac{\Delta p}{p}\,\frac{1}{x'_t}\int_o^{s_t} (x')^2\,ds$$

with $x'_t \equiv \frac{dx}{ds}$ at target, and similar for y. A simple estimate results in

$$(6)\quad \Delta x \sim \alpha \cdot \frac{\varepsilon L}{r_o}\,\frac{\Delta p}{p}$$

with

r_o target radius
L distance F.F.M.-target
ε transverse emittance

The coefficient α exceeds unity for a focusing system with quadrupoles only. Its actual value depends on the first order design and can be minimized according to equ.(5) by an appropriate setting of sufficiently many matching quadrupoles so as to avoid unnecessary fluttering of envelope.

Sextupole correction of chromatic aberrations has not been attempted here, but we have tried to keep $\Delta p/p$ at the level of $\pm$ 0.005 where correction is unnecessary. Due to the variation of space charge defocusing within the bunch and with distance from the target there is concern that sextupoles might do more harm than good if they are used according to concepts developed for high energy beam lines without space charge (Ref.7). Further study is required to clarify sextupole correction in the presence of varying space charge.

According to Ref.8 third order geometric aberrations are tolerable if

$$(7) \quad \varepsilon \lesssim 0.15\, r_o^{5/4}\, \rho^{-1/4}$$

Here ρ is the radius of curvature related to the pole-tip field, and the coefficient 0.15 is about the minimum value that can be achieved by a large class of focusing systems. A brief examination shows that for HIBALL parameters with $\rho \gtrsim 25$ m ($B\rho$ = 106 T-m) the spot size will be spoiled by aberration if ε exceeds in both planes the value 30 mm-mrad. We note that the aberration properties of the Reference Design are very well described by equ.(7) as detailed calculation will show.

References

1. L. Smith et al., LBL-Rep.HIFAN 13-15, Berkeley (1977)

2. I. Haber, IEEE Trans.Nucl.Sci.NS-26, 3090 (1979)

3. I. Hofmann, IEEE Trans.Nucl.Sci.NS-28, 2399 (1981)

4. G. Lambertson et al., IEEE Trans.Nucl.Sci.NS-24, 993 (1977)

5. D. Neuffer, IEEE Trans.Nucl.Sci.NS-26, 3031 (1979)

6. K.G. Steffen, High Energy Beam Optics, Interscience Publishers, New York, 1965

7. K.L. Brown and J.M. Peterson, Proc.of the Heavy Ion Fusion Workshop, Berkeley, Oct.29-Nov.9, 1979, SLAC-PUB-2575 (1980)

8. D. Neuffer, Proc.of the Heavy Ion Fusion Workshop, Argonne, Sept.19-26, 1978, ANL-79-41 (1979)

2. Final Transport and Focusing for HIBALL

2.1 Periodic Transport Lattice for Imploding Bunch

The goal is to transport and simultaneously bunch individual beamlets (20 per cavity) from the accelerator to the target with the following specifications at target:

particle current/beam (averaged over pulse)		1.2 kA
unnormalized emittance	vert.	120 π mm-mrad
	hor.	30 π mm-mrad
momentum spread $\Delta p/p$		± 0.005
pulse length		20 nsec

The requirements to achieve this by ten-fold drift bunching are (see Fig. 2-1.)

initial momentum spread $\Delta p/p$ (coherent + incoherent)		± 0.017
induction linac voltage	~ 300	MeV
length of induction linac	> 150	m
drift distance (induction linac-target)	655	m

There are several options to determine the periodic lattice of these beam lines. The maximum particle current at the end of the periodic lattice is 1.0 kA, assuming a flat pulse shape (note that the final current of 1.2 kA is achieved after drifting through 60 m of large diameter final focusing lenses where space charge is less important). While it is clear from equation (1-1) that quadrupoles at the 1 kA particle current level have to be superconducting (4 T), it appears attractive to divide the lattice at lower currents into sections with normal conducting (< 2 T) and permanent (< 1 T) magnets. The split is performed according to

$$(1) \quad I/q \lesssim 410 \cdot B_Q^{2/3} \quad [A]$$

with an upper limit of 0.3 for $Q'/u_m^{2/3}$ equivalent to a tune of $\sigma_{vert} = 36^o$, $\sigma_{hor} = 18^o$ at the end of each lattice section (see stability discussion in section 1.2). Within a section the lattice is exactly periodic except for the first few magnets that are assumed to perform matching into the changed lattice structure. Details of this lattice are given in Table 2-1.

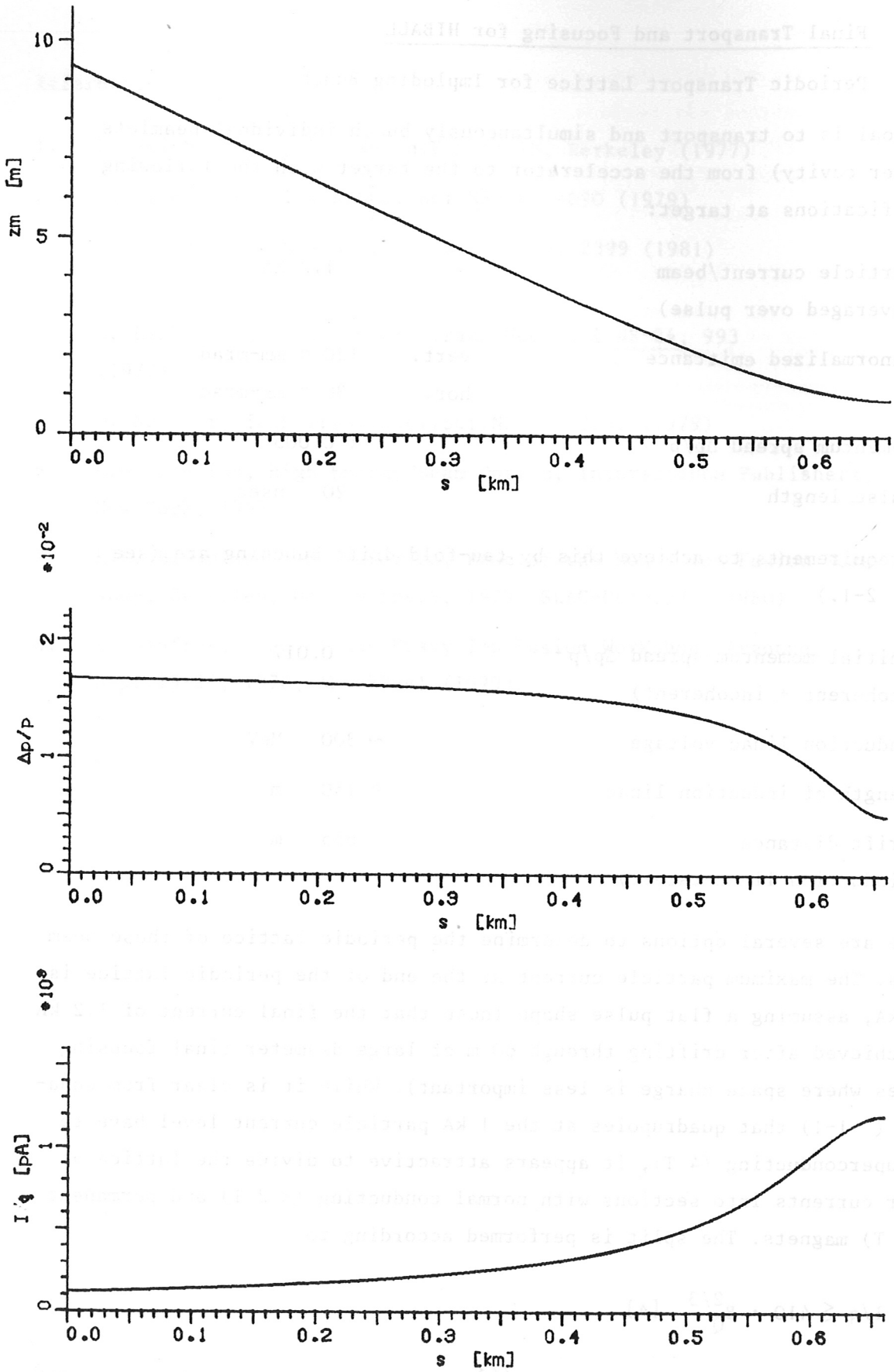

Fig. 2-1. Longitudinal bunch compression by ten-fold drift bunching between induction linac and target. Longitudinal envelope z_m[m], momentum spread $\Delta p/p$ and particle current I/q [kA] according to envelope equation (with g = 2) as function of distance s from induction linac.

Lattice	FODO (symmetric)
occupancy factor	$\eta = \frac{1}{2}$
zero intensity tune	$\sigma_o = 60^o$
tune at max.current in each section	$\sigma_{vert.} = 36^o$, $\sigma_{hor.} = 18^o$
length	595 m
bending radius	150/220 m
average dipole field	0.707/0.482 T

cell	part.current [A]	pole-tip B_Q [T]	max.beam diam.[m]	gradient B_Q/a[T/m]	length of cell [m]
1 - 51 (0 - 415 m)	120 - 350	1	0.102	15.7	8.142
52 - 69 (415 - 508 m)	350 - 560	2	0.082	39.0	5.162
70 - 100 (508 - 595 m)	560 - 1000	4	0.060	133.3	2.790

Table 2-1. Periodic transport lattice for rising beam current. The beam tube diameter is assumed 25% larger than the actual beam diameter.

2.2 Final Focusing - Reference Design

A reference design for the final focusing has been determined along the following lines:

1. In order to keep the beam size and thus second order chromatic and also third order geometric aberrations as small as possible (without correction) the maximum obtainable focusing power is put into the first two quadrupoles, which calls for superconducting magnets. It is assumed that the field at the conductors is limited to 10 Tesla, with a 50 cm thick shield included in the aperture.
2. Matching of the large beam size in the final magnets to the small beam size in the periodic transport is performed as smoothly as possible, searching for a minimum of the integral in equ.(1-5.), which determines the size of chromatic aberrations.

The design has been performed using the computer program SCOP1 (space charge optics program 1) developed at the Max-Planck-Institut für Plasmaphysik. The program has two options:

A. Integration of the Kapchinskij-Vladimirskij envelope equations for first-order design,

B. Raytracing of a random set of trajectories with initial K-V distribution in transverse phase space and square distribution in momentum space. It assumes a linear space charge force derived from the r.m.s. beam envelopes calculated at each time-step. Second order chromatic and third order geometric aberrations can be turned on as well as multipole fields for correction.

Both options use fitting routines for matching (A) and correction (B). Results can be checked with the particle-in-cell code SCOP2 for arbitrary initial distribution with self-consistent space charge force calculation.

First Order Design

The results of a design with hard-edge quadrupoles are shown in Table 2-2 and Fig. 2-2. Note that the first order spot diameter is taken 5 mm to account somewhat for a nonideal beam profile. The plotted beam size has been assumed everywhere 25% larger than the r.m.s. size (K-V envelope) for the same reason.

unnormalized emittance (r.m.s.)	vert. 120 π mm-mrad hor. 30 π mm-mrad (no dilution in periodic transport)
particle current/beam	1.2 kA
first order spot diameter	5 mm
distance F.F.M-target	8.5 m
total length of final focusing	60.374 m
length of quadrupoles	2.683 m
drift sections between magnets	1.789 m
drift section after period.transp.	17.890 m
beam size (1.25 × r.m.s. diameter)	
at exit of periodic transp.	7 × 3 cm
inside front magnet (Q_8)	120 × 60 cm

Gradients [Tesla/m]

Q_1	Q_2	Q_3	Q_4	Q_5	Q_6	Q_7	Q_8	
0.711	4.762	6.561	4.722	1.611	2.868	8.221	7.922	
(F	D	F	D	F	F	D	F	in vertical direction)

Table 2-2 Reference design specifications with hard-edge quadrupoles.

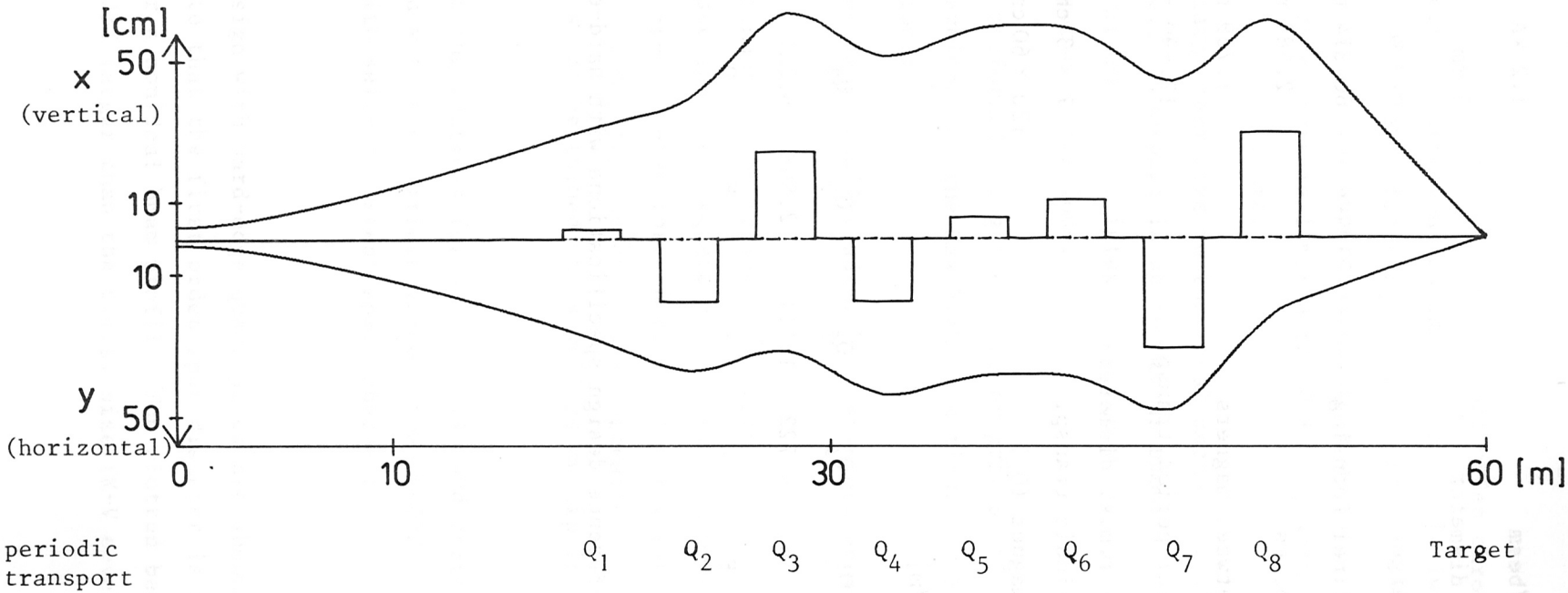

Fig. 2-2 Reference design for final focusing employing 8 quadrupole magnets for beam transfer from the periodic lattice to the target. The square line represents the focusing strength (gradient) in vertical direction.

Higher Order Effects and Beam Characteristics on Target

A distribution of momenta and deviations from paraxial focusing result in an increased spot size. A momentum width of ± 0.005 can be accomodated in the 3 mm radius spot. The situation is different with regard to third order geometric aberrations. Without correction only 40% of the intensity hit the target and it takes a 10 mm radius target to contain 80% of particles, the actual spot being elliptic rather than circular.

Applying fields with octupole symmetry in Q_3, Q_7 and Q_8 has brought some improvement to the degree that a fairly circular spot is obtained with 80% of the particles contained in a radius of 5 mm. This modest improvement might be due to the first order design which does not allow effective (i.e. sufficiently independent) coupling of octupoles to the various aberration terms. In a previous design it has been possible to almost entirely correct aberrations with three octupoles [1], but this design had a larger momentum sensitivity. No attempt has been made to optimize the design for reduced geometric and chromatic aberrations, which will be desirable for future work.

Nonparaxial effects due to a nonuniform space charge have been found in previous work [2] to be comparatively small under similar conditions (similar electric current and beam size, which led to a 20% intensity reduction within the first order spot size).

Summarizing, the presented reference design delivers about 50% (or 40% without octupoles) of the beam intensity on a target with 3 mm radius. The remaining intensity is spread out because of aberrations. Third order geometric aberrations are the dominant constituent; octupoles have been shown to give an improvement at least in principle. The size of the uncorrected aberrations is not discouraging, and it is conceivable that the desired spot can be achieved with improved design.

References

1. I. Hofmann, HIBALL workshop KfK Karlsruhe, Germany, Jan.22-23, 1981

2. I. Bozsik and I. Hofmann, Proc.of the Conference on Charged Particle Optics, Gießen, FRG, 1980, to be published in Nucl.Instr.and Meth.

3. Beam Stripping Theory

3.1 Stripping Cross Section

The total inelastic scattering cross section for Bi^{++} on Pb has been calculated in Born approximation by Y.K. Kim [1]. Following the method described in Reference 2, he has calculated the parameters given in Table 1, which are to be inserted in formulas (1) - (4) of Reference 2. Table 2 gives the atomic properties needed in the calculation. Kim finds

$$\sigma_{in} = 2.2 \times 10^{-16} \text{ cm}^2/\beta^2 \quad .$$

The first order correction to this formula is estimated to be given by the factor [1]

$$1 - 0.002/\beta^2 \quad ,$$

so that the Born approximation should be very good at $\beta^2 = 0.1$. If we assume that the stripping cross section is 1/3 of this, then

$$\sigma_{st} \approx 0.7 \times 10^{-16} \text{ cm}^2/\beta^2 \quad .$$

For $\beta^2 = 0.1$, this is

$$\sigma_{st} \approx 7 \times 10^{-16} \text{ cm}^2 \quad .$$

The best estimate of Pb density in the target cavity when the beam enters is 4×10^{10} atoms/cm^3. This is below the equilibrium density at 470° C which is 8×10^{10} atoms/cm^3. If we take the latter figure as more conservative, we get for the mean free path

$$\ell_{st} \sim 150 \text{ m} \quad .$$

The fraction of beam stripped is

$$1 - \exp(-7 \text{ m}/150 \text{ m}) \sim 5\% \quad .$$

3.2 Beam Loss on Target due to Stripping

Stripping of a beam ion from $q = 2 \rightarrow 3$ results in a larger deflecting force due to the beam space charge. The displacement at target depends on the distance of the projectile from the target as well as from the beam axis at the moment of stripping.

In order to determine what fraction of stripped ions actually miss the target we introduce a loss factor λ in the rate equation

$$(1)\quad d\,n(s) = -\sigma_{st}\,\rho\,n(s)\,\lambda(s)\,ds$$

with ρ the background gas density, n the beam density (atoms/cm^3) and s the distance from target. We have calculated λ for different values of s by tracing trajectories of a randomly distributed set of 100 ions (initial K-V distribution) stripped at distance s and moving under the influence of the space charge force of the focused beam, which results from the zero order envelope motion (see Fig. 3-1). This is valid if only a small fraction of the beam is stripped. By integrating $\lambda(s)$ from 7 m up to the target one finds that the actual loss is only 1/2 the fraction of beam stripped.

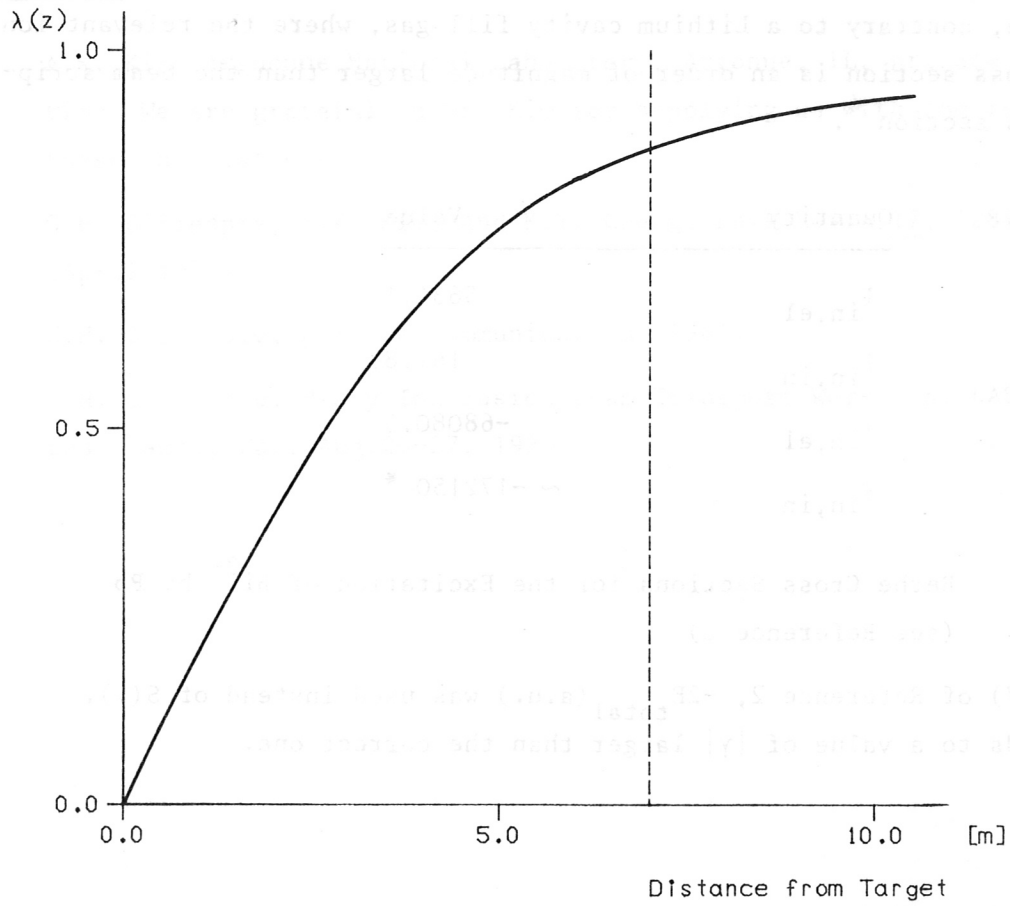

Fig. 3-1 Loss factor $\lambda(s)$ (lost ions/stripped ions) as function of distance from target for HIBALL beam and an assumed K-V transverse distribution.

3.3 Discussion

For the equilibrium density of Pb at 470° C, i.e. 8×10^{10} atoms/cm^3 the predicted stripping is 5% and the loss on target 2.5%. These rates might be up to a factor of two larger if the ratio $\sigma_{st}/\sigma_{in} = 1/3$ is too optimistic. A more accurate calculation of σ_{st} could be carried out by subtracting from σ_{in} the dominant discrete excitations of Bi^{++} by Pb; this would involve several months of computational effort. On the other hand very crude estimates of non-Born corrections suggest a reduction of the cross sections of 20% - 30% at the energy considered [3].

All this amounts to the conclusion that the assumed stripping cross section 7×10^{-16} cm^2 is probably conservative and leads to less than 5% loss for the assumed background gas density.

We note that beam neutralization due to background gas ionization is negligible here, contrary to a Lithium cavity fill gas, where the relevant ionization cross section is an order of magnitude larger than the beam stripping cross section [4].

Quantity	Value
$I_{in,el}$	5634.1
$I_{in,in}$	161.83
$\gamma_{in,el}$	-68080.5
$\gamma_{in,in}$	$\sim$ -172150 *

Table 3-1 Bethe Cross Sections for the Excitation of Bi^{2+} by Pb (see Reference 2)

*In Eq.(17) of Reference 2, $-2E_{total}$(a.u.) was used instead of S(1). This leads to a value of $|\gamma|$ larger than the correct one.

Property *	Bi^{2+}	Pb
Z_N	83	82
Z_e	81	82
$-E_{total}$ (a.u.)	21539.4	20889.3
$\langle r^2 \rangle_{6p} (a_0^2)$	6.914	11.423
$I.P._{6p}$ (eV)	25.08	6.91
$S(-1)$ (Ryd^{-1})	9.433	14.482

Table 3-2 Atomic Properties of Bi^{2+} and Pb

*Based on Dirac-Fock wave functions.

References

1. A.K. Kim, Argnonne National Laboratory, Argonne, IL, private communication. We are grateful to Dr. Kim for supplying us with the results of these calculations.

2. G.H. Gillespie, Y.K. Kim, and K.T. Cheng, Phys.Rev.A 17, 1284 (April 1978).

3. G.H. Gillespie, private communication (1981)

4. G.H. Gillespie, Heavy Ion Fusion Beam Transport Workshop, LASL, Los Alamos, Ca., Aug.26-27, 1980